RESEARCH/REVIEW ARTICLE

Environmental changes during the Paleocene–Eocene Thermal Maximum in Spitsbergen as reflected by benthic foraminifera

Jenö Nagy,[1] David Jargvoll,[1] Henning Dypvik,[1] Malte Jochmann[2] & Lars Riber[3]

[1] Department of Geosciences, University of Oslo, P.O. Box 1047, Blindern, NO-0316 Oslo, Norway
[2] Store Norske Spitsbergen Grubekompani, P.O. Box 613, NO-9171 Longyearbyen, Norway
[3] Weatherford Petroleum Consultants AS, Stiklestadveien 1, NO-7041 Trondheim, Norway

Keywords
PETM; foraminifera; faunal turnover; diversity decrease; sequence stratigraphy.

Correspondence
Jenö Nagy, Department of Geosciences, University of Oslo, P.O. Box 1047, Blindern, NO-0316 Oslo, Norway.
E-mail: jeno.nagy@geo.uio.no

Abstract

The study deals with environmental changes during the Paleocene–Eocene Thermal Maximum (PETM) and its background conditions in Spitsbergen through analysis of benthic foraminiferal assemblages (FA) in a section drilled in the Paleogene Central Basin. The impact of this extreme global warming occurs here in prodelta shelf mudstones composing the lower part of the Gilsonryggen Member (Frysjaodden Formation). The start of the PETM perturbation is marked by a faunal turnover, in which the medium-diversity circumpolar *Reticulophragmium* assemblage was replaced by a low-diversity *Trochammina* fauna. During the hyperthermal period, benthic foraminiferal diversity decreased severely, while the dominance of small-sized taxa with epifaunal morphology strongly increased. This low-diversity fauna occurs in sediments with a reduced thorium/uranium ratio (proxy for oxygenation) and kaolinite enrichment (proxy for high humidity). The faunal changes were thus caused by the combined effects of hypoxic and hyposaline conditions in a stratified water column, due to extreme warming with its accompanying intensified hydrologic cycle. The PETM acme coincides with the maximum flooding surface (MFS) of the Gilsonryggen depositional sequence, composed of the Gilsonryggen Member and the overlying Battfjellet and Aspelintoppen formations. The transgressive phase of the sequence was initiated by local tectonics, while the eustatic sea-level rise of the PETM was superimposed on this transgression.

To access the supplementary material for this article, please see Supplementary files under Article Tools online.

The Paleocene–Eocene Thermal Maximum (PETM) represents the most extreme and rapid global warming during the Cenozoic Era. It was a geologically short period of intense temperature rise, which took place 55.53 million years ago (Westerhold et al. 2009; Charles et al. 2011) and had a striking impact on terrestrial and marine biota (Zachos et al. 2001).

Environmental changes resulting from the PETM are well-documented from low- to mid-latitude sites, where research has long been in progress. Documentation of this hyperthermal in the Arctic marine realm recently started with investigation of drill cores on the Lomonosov Ridge (Pagani et al. 2006; Sluijs et al. 2006) and has been continued in Spitsbergen (e.g., Dypvik et al. 2011; Harding et al. 2011). Assessments of environmental changes in these and related papers are mainly based on proxies derived from geochemical analyses or planktonic microfossils but the biotic response in the benthic realm has not yet been documented.

This study is based on core samples from the borehole Store Norske Spitsbergen Grubekompany (SNSG) BH9/05, located on the eastern flank of the Paleogene Central Basin of Spitsbergen (Fig. 1). The main objective of this article is to delineate the effects of the PETM by means of foraminiferal proxies in the benthic realm of a prodelta succession deposited on the margin of the palaeo-Arctic

Citation: *Polar Research* 2013, *32*, 19737, http://dx.doi.org/10.3402/polar.v32i0.19737

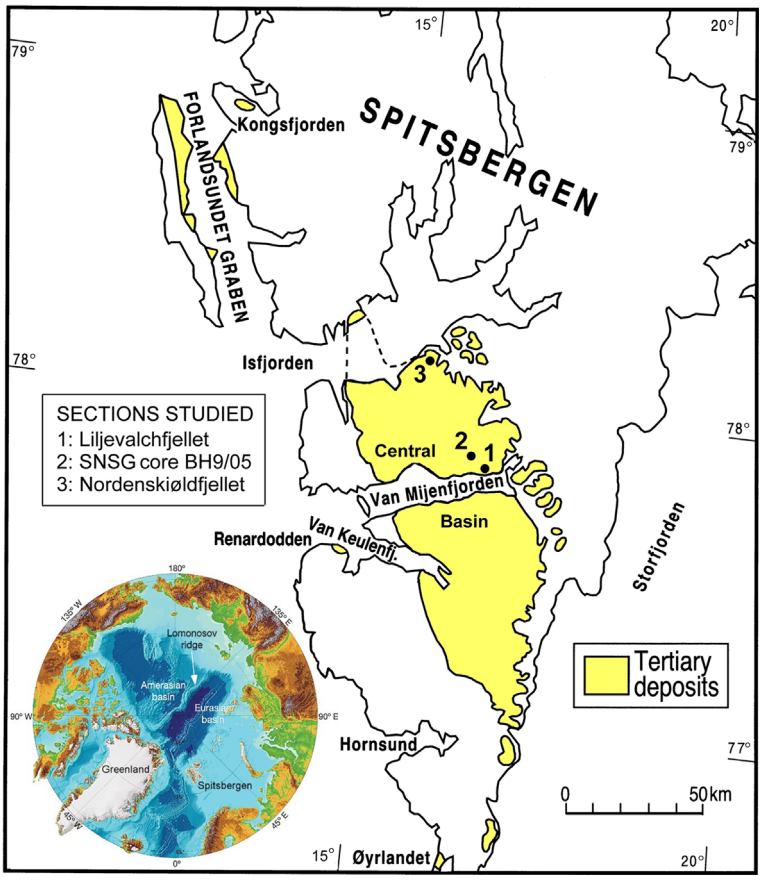

Fig. 1 Position of the Palaeogene Central Basin of Spitsbergen and location of the studied sections. Spitsbergen is the main island of the Svalbard Archipelago. This article is based on the Store Norske Spitsbergen Grubekompany (SNSG) core section BH9/05.

Ocean. It also aims to consider the PETM impact in a transgressive–regressive context. This is the first documentation of the response of bottom-dwelling biota to the PETM in the Arctic.

Global effects of the PETM

The PETM hyperthermal period lasted 150 000–220 000 years (Röhl et al. 2007; Aziz et al. 2008) and was superimposed on the already warm ("greenhouse") climate of the Paleogene Epoch, which was pronounced in the Arctic (Moran et al. 2006). At several sites globally, the warming shows an abrupt onset, sharp peak and a gradual long-term recovery (Zachos et al. 2001).

The temperature rise during the PETM is displayed by a prominent negative $\delta^{18}O$ excursion ($>1‰$) in benthic and planktonic foraminiferal calcite, and in palaeosol carbonates (Thomas & Shackelton 1996; Magioncalad et al. 2004).

Information about components of the global carbon reservoir is obtained by carbon isotope analyses of foraminiferal calcite or the organic carbon content of sediments. The PETM is characterized by a sudden negative $\delta^{13}C$ excursion of ca. 3‰ of the global carbon reservoir (Kennett & Scott 1991), evidencing an abrupt release of isotopically light carbon into the ocean–atmosphere system, thus a rise in the "greenhouse" gas concentration. It may have originated from dissociation of isotopically light methane from shallow sub-seabed clathrates, with subsequent oxidation to carbon dioxide (Dickens et al. 1995; Bowen et al. 2004). But alternatively, huge quantities of greenhouse gases may have been produced by the release of carbon compounds in the Norwegian Sea, associated with extensive volcanic intrusions in organic-rich sediments (Svensen et al. 2004). Other theories are outlined by Alegret et al. (2010).

In the deep sea, the hyperthermal led to a 5–6°C bottom-water temperature rise (Thomas & Shackelton 1996). The sea-surface temperature increased by 8°C at high latitudes and to a lesser degree towards lower latitudes (Kennett & Scott 1991; Kelly et al. 1996).

Citation: *Polar Research* 2013, *32*, 19737, http://dx.doi.org/10.3402/polar.v32i0.19737

In the Arctic, sea-surface temperatures increased by ca. 5°C (Sluijs et al. 2006). A significant global rise of the carbonate compensation depth (CCD) led to extensive dissolution of seafloor carbonates (Thomas et al. 1999).

The biotic responses to the PETM include: severe extinction of calcareous benthic foraminiferal taxa (Thomas 1998); extensive radiation of exotic planktonic foraminiferal taxa (Kelly et al. 1996); among deep-water agglutinated foraminifera, a widespread boom of the opportunistic genus *Glomospira* (Galeotti et al. 2004; Kaminski & Gradstein 2005); global bloom and northward migration of the dinocyst *Apectodinium augustum* (Crouch et al. 2001); migration of land plants (Wing et al. 2005) and mammals (Smith et al. 2006) to higher latitudes. The long-term recovery may have been associated with an increase in marine productivity and influx of organic carbon (Zachos et al. 2001).

The Spitsbergen Paleogene succession

The Central Basin, with the studied core section, is a large structural depression occupying most of the southern part of Spitsbergen (Fig. 1). The Paleogene sediment infill of the basin is ca. 2.3 km thick, widely exposed and ranges in age from Paleocene to Eocene but may also include Early Oligocene strata. It consists mainly of siliciclastic mudstones and sandstones deposited in fluvial, deltaic to delta-influenced marine shelf environments. The Tertiary tectonostratigraphic development of Spitsbergen is outlined by Steel et al. (1985) and Harland (1997).

The Central Basin succession is subdivided into six formations (Dallmann et al. 1999), which in this article are arranged into four depositional sequences (Fig. 2). The sequences are named after the lithostratigraphic unit containing the maximum flooding surface (MFS) and are outlined below (in ascending order).

(1) The Kolthoffberget Sequence rests on a regional unconformity with an associated hiatus spanning the Late Cretaceous. The sequence starts with delta plain mudstones and sandstones, culminates with maximum flooding in prodelta mudstones and terminates with delta front sandstones of the Endalen Member. (2) The Basilika Sequence starts with delta front sandstones,

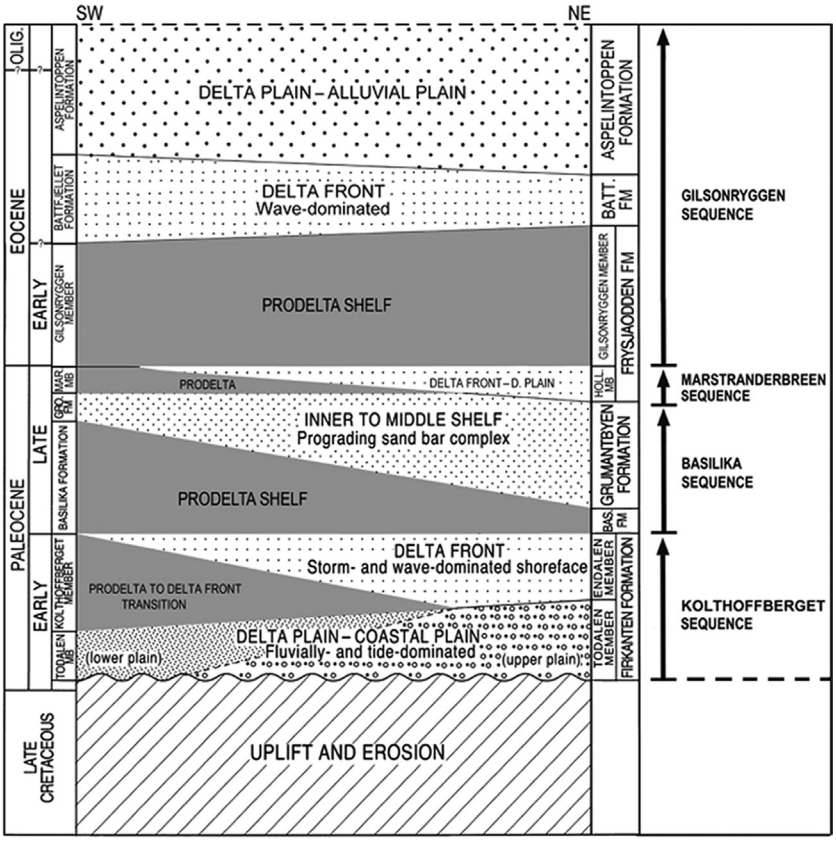

Fig. 2 Stratigraphic outline showing the sedimentary infill of the Paleogene Central Basin of Spitsbergen with subdivision into four depositional sequences.

attains maximum flooding in prodelta shelf mudstones and ends with the shelf sand bar complex of the Grumantbyen Formation. (3) The thin Marstranderbreen Sequence culminates in prodelta mudstones and ends with delta plain sandstones of the Hollendardalen Member. (4) The Gilsonryggen Sequence commences with shoreline deposits, culminates in prodelta shelf mudstones, continues in delta front sandstones and terminates in delta plain to alluvial plain sandstones and mudstones of the Aspelintoppen Formation.

Recognition of the Spitsbergen PETM

The PETM occurs in the lowermost part of the Gilsonryggen Sequence, coinciding with the maximum flooding interval of this sequence (Fig. 2). An important contribution to recognition of the PETM at this level was provided by Manum & Throndsen (1986), who defined the Paleocene–Eocene transition by discovering a dinocyst assemblage containing the global indicator of the PETM, *A. augustum* in the Nordenskiøldfjellet section.

Recent studies of the Paleogene "greenhouse" period in Spitsbergen were conducted within the paleo-Arctic Climates and Environments (pACE) project co-operation, which also included an early phase of this study. The first results of the pACE initiative concerning the Spitsbergen PETM have been published in several conference abstracts (e.g., Dypvik et al. 2010; Nagy, Dypvik et al. 2010). More comprehensive results have been presented by: Harding et al. (2011), focusing on carbon isotope and plankton (dinocyst) distribution data; Dypvik et al. (2011), dealing with mineralogical and geochemical features; Charles et al. (2011), providing new numerical age constraints; Cui et al. (2011), presenting a detailed carbon isotope curve and discussing the PETM release rate of fossil carbon into the ocean–atmosphere system. The last four papers deal with core BH9/05, for which this study provides benthic biotic data.

Background environments of the Spitsbergen PETM

A brackish palaeo–Arctic Ocean

In Paleocene–Eocene times, the Arctic Ocean formed a semi-enclosed basin, due to the absence of a deep-water communication between the Polar Basin and the world ocean (Briggs 1987; Harland 1997; Ogawa et al. 2009). Based on foraminiferal studies in the Canadian Arctic, McNeil (1990) introduced the term "Arctic Gulf" to emphasize the restricted nature of this ocean basin, which formed a Boreal biogeographic province. Additional evidence demonstrating the circum-Arctic extent of this province was provided by Podobina (2000) from western Siberia and by Nagy (2005) from Spitsbergen. Salient features of the Arctic Gulf were low salinity and high carbonate-corrosivity. These factors acted as severe barriers for calcareous benthic foraminifera, and excluded planktonic taxa, but favoured development of low- to medium-diversity agglutinated assemblages of endemic composition.

Basic information on the Paleocene–Eocene evolution of the Arctic Ocean, including the Boreal PETM, is provided by data from IODP core site 302 located on the Lomonosov Ridge (Moran et al. 2006). Organic geochemical data based on core 302-4A indicate that the Arctic sea-surface water temperatures during the PETM increased from 18°C in latest Paleocene to ca. 23°C, and then decreased to ca. 17°C at the end of the hyperthermal event (Sluijs et al. 2006). During this period of intensive warming, a sudden influx of the subtropical dinocysts *Apectodinium* spp. occurred. Thus, data from the Lomonosov Ridge support the generally held view that the Paleogene greenhouse world was free of polar ice sheets.

In core 302-4A, high frequency of the dinocysts *Senegalinium* spp. and *Cerodinium* spp. indicates low surface water salinities (Sluijs et al. 2006), which coupled with geochemical data and abundant terrestrial organic matter suggest a core position proximal to a deltaic coastline. The presence of laminated sediments and increased isorenieratene contents indicate bottom-water hypoxia. It implies an intensive thermohaline stratification of the water column owing to high freshwater influx combined with increased temperatures, and amplified by the semi-isolated nature of the Paleogene Arctic Ocean. Brackish to even freshwater conditions seem to have been normal of this ocean during Paleocene–Eocene times. A peak of oceanic freshening appeared at the onset of the Middle Eocene (ca. 49 million years ago), signalled by the boom of the floating freshwater fern *Azolla* recognized in the Lomonosov Ridge core 302-4A (Brinkhuis et al. 2006).

The PETM of the Lomonosov Ridge and the Central Basin was superimposed on the overall restricted conditions of the palaeo-Arctic Ocean. By Early Miocene times, a deep-water connection with the North Atlantic was established by seafloor spreading between Spitsbergen and Greenland, leading to the development of normal marine salinity and oxygen in the Arctic Ocean (Jakobsson et al. 2007), as well as an influx of deep-water agglutinated foraminifera from the North Atlantic (Kaminski et al. 2009).

Citation: *Polar Research* 2013, *32*, 19737, http://dx.doi.org/10.3402/polar.v32i0.19737

Significance of the Spitsbergen Paleogene deltas

The overall environmental conditions of the palaeo-Arctic Ocean are reflected in the sedimentary infill of the Spitsbergen Central Basin, but modified by extensive local deltaic developments. Freshwater discharge from the Spitsbergen deltas might have contributed significantly to the reduced salinity and carbonate-starved nature of the Paleogene Arctic Basin.

The main manifestation of this freshwater source is the impact of delta plain conditions at four levels of the Spitsbergen succession: the Todalen and Endalen members (of the Firkanten Formation), the Hollendardalen Member (of the Frysjaodden Formation) and the Battfjellet–Aspelintoppen formations (Fig. 2). The four intervening shale–siltstone-dominated intervals are of prodelta to prodelta shelf origin: the Kolthofberget Member (of the Firkanten Formation), the Basilika Formation, the Marstranderbreen Member (of the Frysjaodden Formation) and the Gilsonryggen Member (of the Frysjaodden Formation). The total organic carbon (TOC) content of the succession is intermediate (average 1.1%), while the overall calcium carbonate content is extremely low (average 0.4%).

The foraminiferal assemblages (FA) of the Central Basin succession consist of agglutinated taxa, except for a few horizons containing calcareous benthic forms in very low amounts (Nagy et al. 2000; Nagy 2005; Rüther 2007). The species diversities are low with average alpha 2.3, and the assemblages are of circumpolar type, endemic to the Arctic. The assemblages indicate that low salinity and locally low oxygen content were the main restricting factors in the thermohaline-stratified water column of the Central Basin.

Materials and methods

The analysed sediment core, BH9/05 was drilled by SNSG when conducting exploration of coal resources in the northern part of the Central Basin (Fig. 1). The sedimentary logs and sample set from the core were also used by Dypvik et al. (2011), Charles et al. (2011) and Cui et al. (2011). To delineate biofacies changes, we used benthic foraminiferal species distribution, faunal diversity pattern, test size variation and morphogroup (MG) analysis.

Logging, sampling and laboratory treatment

Logging and sampling of core BH9/05 were undertaken in the summer of 2008 in the core storage premises of SNSG, close to Longyearbyen. Lithology and sedimentary structures were logged from 547 to 111 m at a scale of 1:50. The interval containing the PETM from 560 to 547 m was logged at a scale of 1:20. For foraminiferal analyses, a series of 66 mudstone samples were selected to cover the Gilsonryggen Member, most densely at and around the PETM.

All processed samples contained foraminifera, but in varying abundance. The assemblages are entirely agglutinated, except for a few samples containing calcareous forms in very low amounts. Almost all foraminiferal tests are compressed owing to high degree of initial soft sediment compaction.

The sampled mudstones and shales are strongly lithified. For extraction of foraminifera, the tenside method was initially attempted according to the procedure described by Nagy (2005). The method failed to disintegrate the sediment sufficiently, owing to the high degree of cementation. We therefore switched to the kerosene method, which gave adequate results. In the kerosene method (as in the tenside procedure), the first step is to crush the dried samples into pieces of about 0.5 cm^3. The sediment is then soaked in kerosene for 30 min. After decanting the kerosene, about 15 g of sodium hydroxide (NaOH) is added to 50 g of sediment in a 1:3 sediment-to-water mixture. Then the mixture is boiled for 30 min. If necessary, the procedure is repeated. Extended boiling has to be adjusted to the degree of sediment cementation because the sodium hydroxide may corrode poorly cemented foraminiferal tests.

After disintegration, the samples were washed through sieves with mesh diameters of 63, 90, 125 and 500 μm. The fractions from 90 to 500 μm were used in the foraminiferal analyses. The fraction above and below this interval contained no identifiable foraminifera. From the sieved residues, on average 150 foraminiferal tests per sample were picked for further analysis (Supplementary File).

Faunal diversity

The alpha diversity index combines the number of individuals and number of species per sample, and allows comparison of samples of different sizes (Murray 1973). It is based on the assumption that there is a logarithmic relationship between the number of individuals and number of species in an assemblage.

The Shannon–Weaver diversity index [H(S)] is based on the information function and was originally applied to foraminifera by Buzas & Gibson (1969). It takes into account both the number of species and their relative frequency (evenness), thus this is a diversity-dominance index. When all species in an assemblage have equal relative abundance, a maximum value for H(S) is achieved.

Plots of the alpha index against H(S) are used to characterize faunas of modern environments (Murray 2006) and to interpret the facies of ancient assemblages (Nagy et al. 2011).

Test size analysis

The foraminiferal size analysis was done in the following steps: (1) measuring the dimensions of at least 150 tests per species under a binocular microscope, except for less-abundant species where all tests were measured; (2) arranging species into categories according whether they were subcircular, subelliptical or subtriangular in shape; (3) calculating the average surface area for each species expressed as upper + lower surface (because the tests are compressed); (4) arranging species into four size groups; (5) calculating the percentages of the size groups in each sample, based on the percentage frequency of the species. This procedure gives only approximate results owing to the compressed nature of the tests, but appears sufficient to delineate test size trends within the analysed section (Fig. 7).

MG analysis

The idea of combining foraminiferal taxa into morphological categories, then applying these to environmental assessments is based on the assumption of a relationship between test shape, function and habitat. The approach used in this study follows the lead of Jones & Charnock (1985), who integrate test shape, life position and feeding strategies to define MGs in modern agglutinated faunas. A modified version of this concept was transferred to Jurassic assemblages by Nagy (1992) and is applied in this study (Fig. 8).

Sedimentary succession of core section

The analysed interval of core BH9/05 comprises the uppermost part of the Grumantbyen Formation and the entire Frysjaodden Formation, as at this site the Frysjaodden is represented only by the Gilsonryggen Member (Fig. 3), while the lower two members of the formation (the Marstranderbreen and Hollendardalen) cannot be recognized. This is usually the case in eastern parts of the Central Basin, where the Gilsonryggen Member rests directly on the Grumantbyen Formation.

Grumantbyen Formation (560–552 m)

Only the topmost part of this formation is included in the analysed core section (Fig. 3). It consists mainly of very fine-grained greenish grey sandstones with subordinate amounts of mudstone. Chlorite and glauconite are typical constituents. The sediment is heavily bioturbated, leaving only a few laminated layers and some ripple marks intact. More than 80% of the trace fossils are horizontally oriented and mostly are of *Planolites* type. Only a few high-angle burrows occur.

Gilsonryggen Member of the Frysjaodden Formation

Transitional beds (552–533 m). A conglomerate bed at 552 m marks the lower boundary of the Gilsonryggen Member (Frysjaodden Formation). The basal 3 m of the member consists of siltstone and fine-grained sandstone beds (comprising ca. 25%), alternating with dark shales (Fig. 3). This segment contains a few scattered bioturbation traces and a thin conglomeratic horizon at 549 m. The interval as a whole reveals a generally upwards-fining development accompanied by upwards-increasing TOC content varying from 0.7 to 2.9%. The shale contains subspherical pyrite concretions up to 1 cm in diameter. From 535 to 533 m, the shale becomes more greyish and contains three siderite interbeds (2–3 cm in thickness).

Lower shales (533–344 m). This interval consists of dark grey non-bioturbated shales with very low silt content and TOC varying from 0.8 to 1.4%. Fine lamination is common at numerous horizons, and scattered pyrite concretions (diameter of 3–8 mm) are present throughout (Fig. 3). Up to 1 cm thick plastic clay beds, possibly bentonites, occur at 517 and 511 m. From 500 m upwards, chert pebbles appear occasionally and are interpreted as dropstones transported on the thalli of floating seaweed. Siderite-cemented beds up to 1 cm thick appear at 500 m, and increase in frequency and thickness upwards. Decimetre-thick silty beds are typical for the upper part of the interval.

Middle shales (344–166 m). This unit consists of shales with subordinate siltstones and sandstones mainly concentrated in the upper part. The TOC content varies from 0.7 to 1.9%. In its lower part (up to 242 m), there is a very weak coarsening-upwards, as seen in the increasing number and thickness (up to 1 dm) of silt horizons. The silts are grey to reddish, and may represent distal hyperpycnites or storm beds. They usually contain dense bioturbation consisting of Chondrites-type traces ca.1 mm in diameter. Above 256 m, the interval is typified by several large-scale coarsening-upwards and fining-upwards parasequences (Fig. 3) containing fine sand in their

Citation: *Polar Research* 2013, *32*, 19737, http://dx.doi.org/10.3402/polar.v32i0.19737

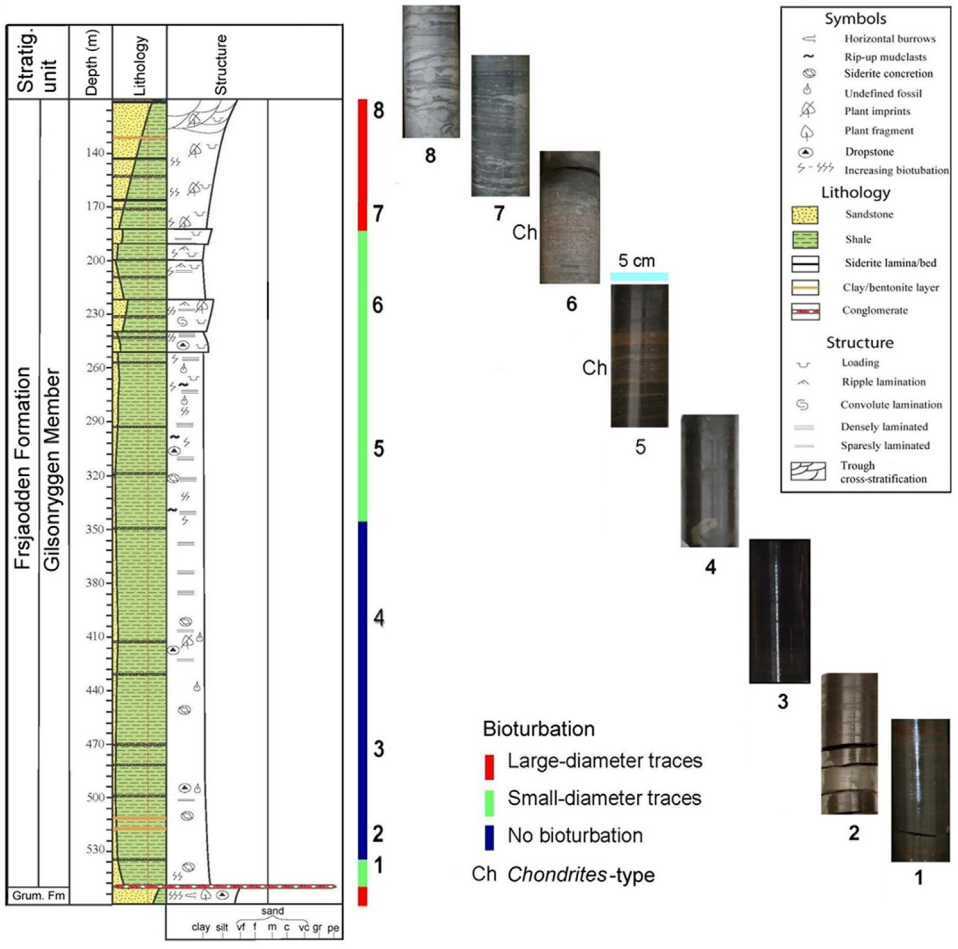

Fig. 3 Lithological column of the analysed Gilsonryggen Member (Frysjaoden Formation) logged in core BH9/05, with bioturbation trends illustrated by core pieces numbered to show their stratigraphic positions.

coarsest parts. Load structures are frequent, sometimes in combination with convolute lamination, suggesting high sedimentation rates. Hummocky cross-stratification is present, while ripple lamination is abundant. Silty horizons with small-diameter trace fossils are typical also at these levels.

Uppermost sandy beds (166–111 m). These sandstones and shales form an overall coarsening-upwards succession, with sand content up to 95% at 111 m. The TOC content of shale horizons ranges from 1.8 to 2.1%. Hummocky cross-bedding, wave-generated ripple lamination and load structures are common, with trough cross-bedding appearing in the upper parts. Dominantly large-diameter bioturbation traces are abundant, particularly in the mixed sand/shale segments. The traces are mainly horizontal and increase in diameter upwards. The top of the interval represents the boundary with the sandstones of the overlying Battfjellet Formation.

Biofacies changes at the PETM and in adjacent strata

Through the Gilsonryggen Member, the stratigraphic distribution of foraminiferal taxa, their diversity, MG distribution and test size show changes of varying magnitude attributed to changing environmental conditions (Figs. 4, 5; Supplementary File). The most pronounced changes are associated with the PETM. The faunal succession of the member is subdivided into four FA, one below, one within and two above the hyperthermal event.

The foraminiferal succession

***Reticulophragmium* assemblage, FA 1.** This pre-PETM assemblage is typical for the lowermost part of the

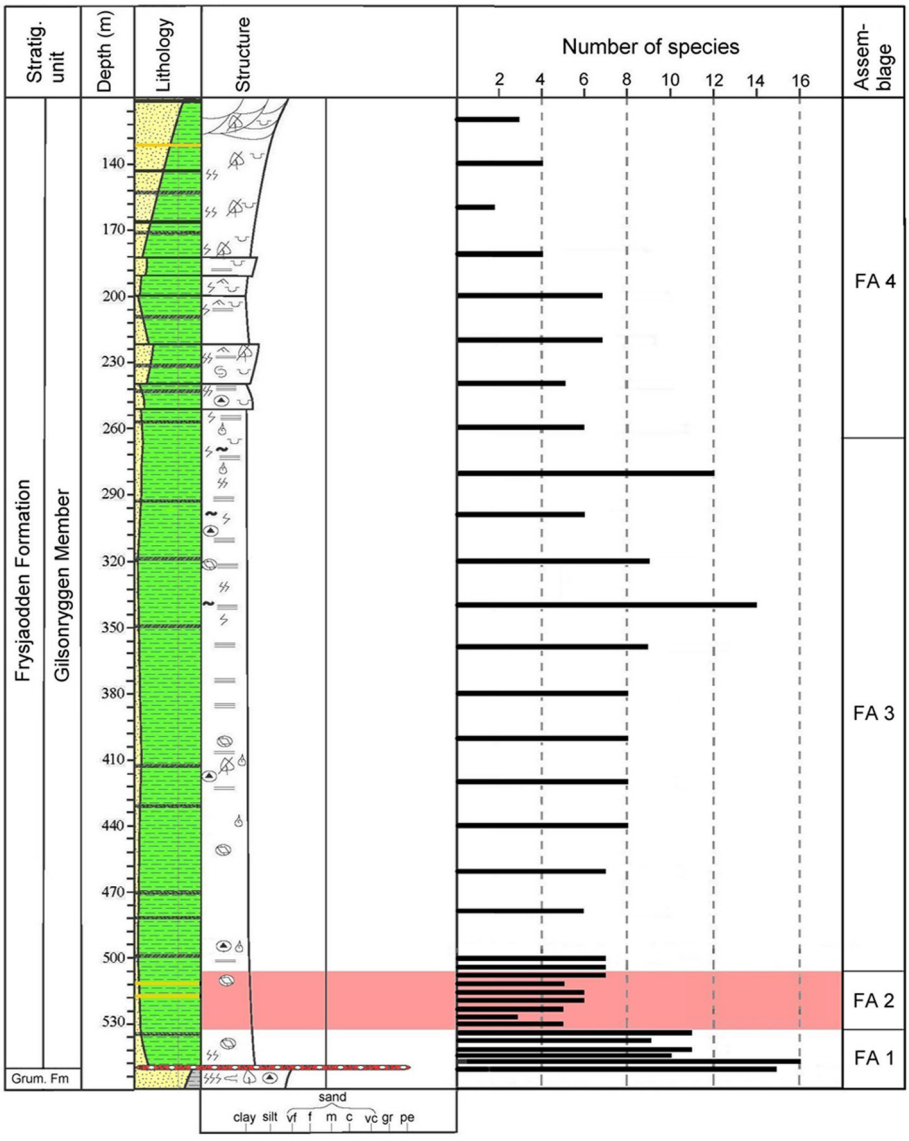

Fig. 4 Foraminiferal diversity portrayed as the number of species in core BH9/05 and subdivision into four assemblages. The Paleocene–Eocene Thermal Maximum (PETM) anomaly is marked with red shading.

Gilsonryggen Member, recognized from 549.75 to 534.37 m in core BH9/05 as well as in corresponding basal shales of the Nordenskiøldfjellet section. Characteristic species include *Reticulophragmium arcticum, Reticulophragmium borealis and Labrospira turbida*. A few calcareous species, including *Nonion* aff. *insolitum* and *Cibicidoides* aff. *diuturnis,* occur sporadically. The sudden disappearance of this assemblage defines the faunal turnover marking the base of the PETM (Fig. 5).

***Trochammina* assemblage, FA 2.** This assemblage occurs above the faunal turnover from 532.37 to 506.05 m and is associated with the PETM anomaly. It is strongly dominated by *Trochammina* aff. *inornata*. Other common species include *Thurammina* aff. *papillata, Birsteiniolla* sp. 1, *Trochammina tagluensis* and *Verneuilinoides* aff. *exvadum* (Fig. 5). The three most common species also occur below the faunal turnover, although in much smaller amounts.

***Repohax* assemblage, FA 3.** This is the first post-PETM assemblage and is recognized from 504.05 to 260.05 m. It is characterized by the common occurrence of *Reophax* aff. *metensis*. Other frequent species include *Trochammina* aff. *inornata* and *Thurammina* aff. *papillata*.

Citation: *Polar Research* 2013, *32*, 19737, http://dx.doi.org/10.3402/polar.v32i0.19737

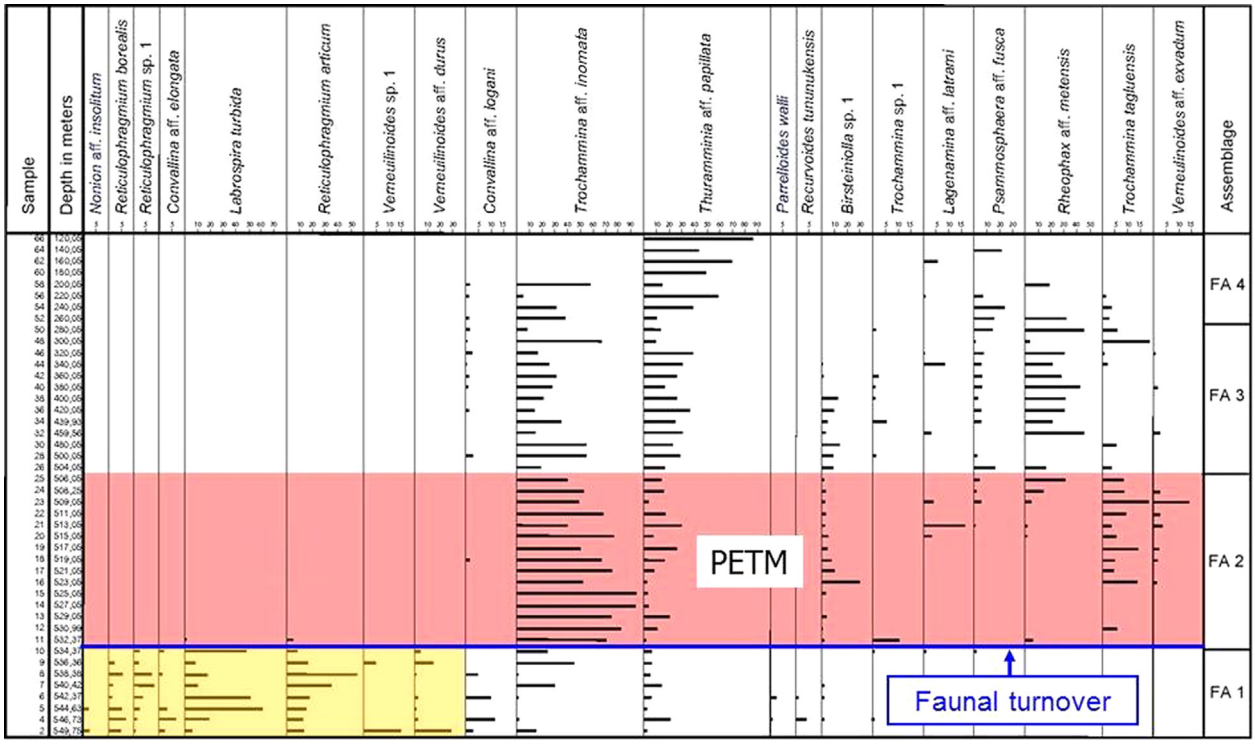

Fig. 5 Distribution of 20 foraminiferal species in core BH9/05. The Paleocene–Eocene Thermal Maximum (PETM) anomaly with a faunal turnover at its base is indicated, and the assemblage subdivision is marked. A total of 18 rare species are omitted.

Less common but typical species are *Psammosphaera* aff. *fusca* and *Birsteiniolla* sp. 1.

***Thurammina* assemblage, FA 4.** The second post-PETM assemblage is found from 240.05 to 120.05 m (Fig. 5). It shows a high dominance of *Thurammina* aff. *papillata* with locally common *Psammosphaera* aff. *fusca* and *Trochammina* aff. *inornata*. Rare calcareous species as *Melonis* aff. *affinis* and *Nonion* sp. occur in a few samples.

Faunal diversities

The three diversity proxies, number of species, H(S) and alpha index, show essentially similar trends through the analysed section (Figs. 4, 6, 11). Below the PETM, through the interval from 549.8 to 534.4 m, the number of species per sample varies from 9 to 15 and the H(S) from 1.4 to 2.3. Both proxies show an upwards-decreasing distribution trend.

The PETM anomaly, in the interval from 533.4 to 508.3 m, is characterized by strongly reduced diversity values: the number of species ranges from 3 to 7 and the H(S) varies from 0.3 to 1.6.

Above the PETM, through the 505 to 360 m interval, the number of species per sample varies between 6 and 9 and the H(S) from 1.2 to 1.6. Post-PETM diversity maxima occur between 340 and 280 m, where the species number reaches 14 and an H(S) attains 1.9. This is followed by upward-decreasing diversities between 260 and 120 m typical for the upper part of the Gilsonryggen Member, with number of species varying from 2 to 7 and H(S) between 0.2 and 1.4.

Size variation of foraminifera

Test outline categories. For measurement of dimensions and subsequent calculation of test surface areas, the species are arranged into three test outline groups by relating the shapes of the compressed tests to circles, ellipses and triangles (see methods section). The most common taxa exemplifying these categories are: (1) subcircular: *Trochammina* aff. *inornata, L. turbida, R. arcticum, T. tagluensis, Psammosphaera* aff. *Fusca;* (2) subtriangular: *Verneuilinoides* aff. *durus, Reophax* aff. *metensis, Convallina* aff. *logani;* (3) subelliptical: *Birsteiniolla* sp. 1, *Lagenammina* aff. *lathrami, Miliammina* sp.

Test surface area categories. The diagrammatic presentation of foraminiferal size distribution through the analysed section is based on categorizing species

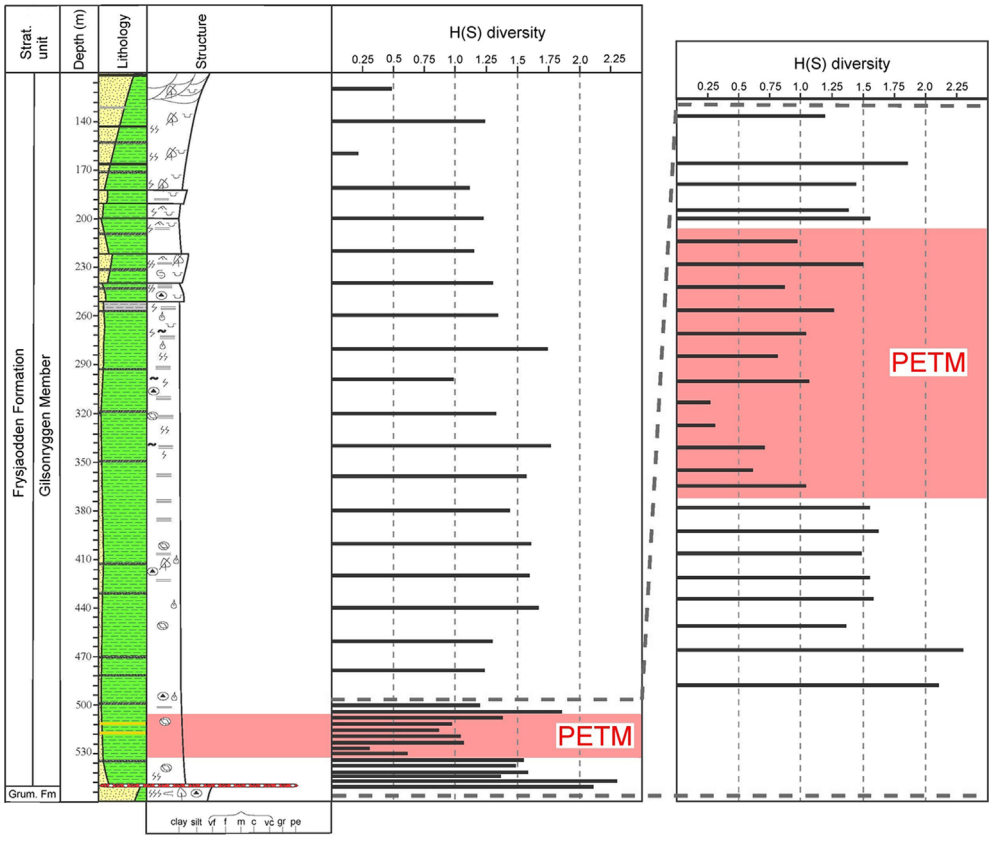

Fig. 6 Distribution of the H(S) diversity index of foraminifera in core BH9/05. The lowermost part of the Gilsonryggen Member with the Paleocene–Eocene Thermal Maximum (PETM) anomaly is also shown at an expanded scale.

into the following four surface area groups (SAG), the stratigraphic distribution of which is displayed in Fig. 7.

SAG-1, range 0.04–0.07 mm^2: *Reticulophragmium* sp. 1, *Verneuilinoides* sp.1, *Trochammina* aff. *inornata*, *Birsteiniolla* sp. 1, *Lagenammina* aff. *lathrami*, *Verneuilinoides* aff. *exvadum*, *Ammodiscus macilentus*, *Gravellina* aff. *dawsoni*, *Ammomarginulina* aff. *brevis*.

SAG-2, range 0.07–0.14 mm^2: *L. turbida*, *Verneuilinoides* aff. *durus*, *Convallina* aff. *logani*, *Thurammina* aff. *papillata*, *Trochammina* sp. 1, *Psammosphaera* aff. *fusca*, *Glomospirella* aff. *gordialiformis*, *Recurvoides tununukensis*, *Hyperammina* sp., *Ammobaculites* sp., *Glomospirella* sp.

SAG-3, range 0.14–0.28 mm^2: *Convallina* aff. *elongata*, R. *arcticum*, *Reophax* aff. *metensis*, *T. tagluensis*, *Miliammina* sp.

SAG-4, range 0.28–0.40 mm^2: *R. borealis*, *Calamopsis* sp.

Stratigraphic size distribution patterns. In core BH9/05, the lowermost part of the Gilsonryggen Member from 549.8 to 534.4 m (i.e., the interval below the PETM) is dominated by SAG-2 and -3 with maximum values of 70 and 69%, respectively. SAG-4 is restricted to this interval, but its maximum is only 8%, in contrast to the dominant impression given under the microscope by the robust *R. borealis* that typifies this SAG. The group comprising the smallest tests, SAG-1, has its minimum abundance of 3% in this interval (Fig. 7).

In the PETM anomaly, from 533.4 to 508.3 m, the smallest sized SAG-1 is heavily dominant with peak values of 95 and 82%. The groups of larger sizes, SAG-2 and -3, are reduced to a minimum of 3% and are even absent in one sample.

Above the PETM, through the interval from 505 to 400 m, SAG-1, -2 and -3 occur in varying abundance within the following ranges: SAG-1, 20–72%; SAG-2, 23–45%; SAG-3, 1–45%. The percentage of SAG-1 generally decreases upwards.

Foraminiferal MGs

To palaeoenvironmental assessments, the most important contribution of the MG approach is information concerning recognition of benthic microhabitats (Nagy et al. 1995; Reolid et al. 2008; Setoyama et al. 2011). Modern

Citation: *Polar Research* 2013, *32*, 19737, http://dx.doi.org/10.3402/polar.v32i0.19737

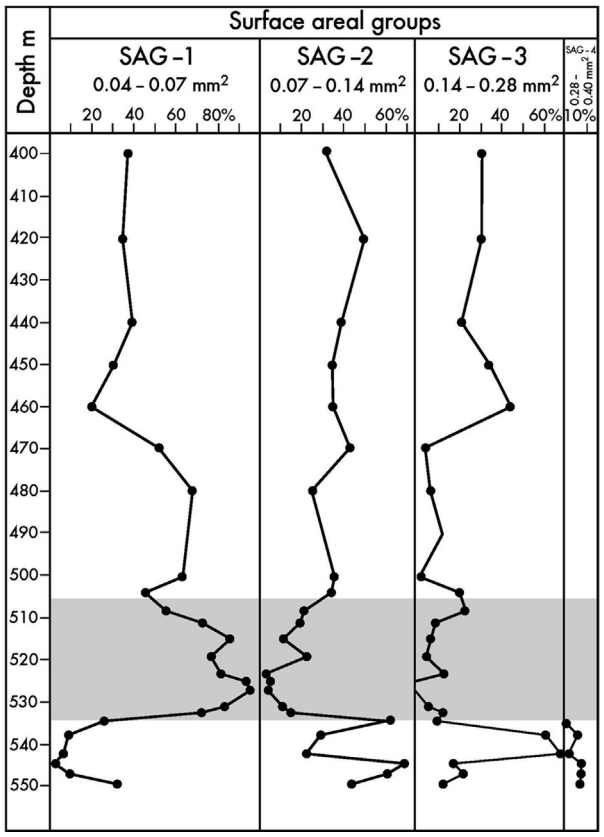

Fig. 7 Distribution of foraminiferal test surface area groups (SAG) in the lower 150 m of core BH9/05. The Paleocene–Eocene Thermal Maximum (PETM) anomaly (shaded) is characterized by reduced test dimensions shown by the high dominance of SAG-1.

and fossil agglutinated foraminifera partition their environment vertically into several separate niches. The environmental conditions in these microhabitats are defined by a combination of several factors, the relative importance of which is expressed by the MG distribution pattern. One of the most crucial is oxygenation of the bottom-water and the pore water of the underlying sediment (Jorissen et al. 1995). Other important factors include food supply, water depth and current activity.

MG composition. In the analysed section, six MGs are distinguished based on inferred microhabitat preferences. The taxonomic composition of the groups is outlined below, and their stratigraphic distribution displayed in Fig. 8.

MG-1, Erect: *Hyperammina* sp.

MG-2, Epifaunal: *Birsteiniolla* sp., *Ammodiscus* aff. *macilentus*, *Glomospira* sp. *Glomospirella* aff. *gordialiformis*.

MG-3, Surficial: *Trochammina* aff. *inornata*, *Trochammina* sp. 1, T. *tagluensis*.

MG-4, Semi-immersed: *Thurammina* aff. *papillata*, *Psammosphaera* aff. *fusca*.

MG-5, Semi-infaunal: *R. borealis*, *Reticulophragmium* sp. 1, *L. turbida*, *R. arcticum*, *Recurvoides tununukensis*, *Miliammina* sp.

MG-6, Infaunal: *Convallina* aff. *elongata*, *Verneuilinoides* sp.1, *V.* aff. *durus*, *Convallina* aff. *logani*, *Lagenammina* sp., *L.* aff. *lathrami*, *Reophax* aff. *metensis*, *Ammomarginulina* aff. *brevis*, *Ammobaculites* sp., *Verneuilinoides* aff. *exvadum*.

MG distribution patterns. The pre-PETM deposits comprising the lowermost part of the analysed core (from 549.8 to 534.4 m), are typified by the semi-infaunal group MG-5 occurring with frequencies from 29 to 85% (Fig. 8) and dominance of *R. arcticum* and *Labrospira turgida*. Three other groups are common with the following maximum frequencies: MG-3, 46%; MG-4, 14%; MG-6, 49%.

The interval from 534.4 to 504 m, comprising the PETM anomaly, is strongly dominated by the surface-dwelling group MG-3 with frequencies from 44 to 94%. The group is made up of species belonging to *Trochammina,* mainly *T.* aff. *inornata.* The semi-immersed group MG-4 is common in most samples with varying frequency from 2 to 31% and dominance of *Thurammina* aff. *papillata.* The infaunal group MG-6 is rare to absent

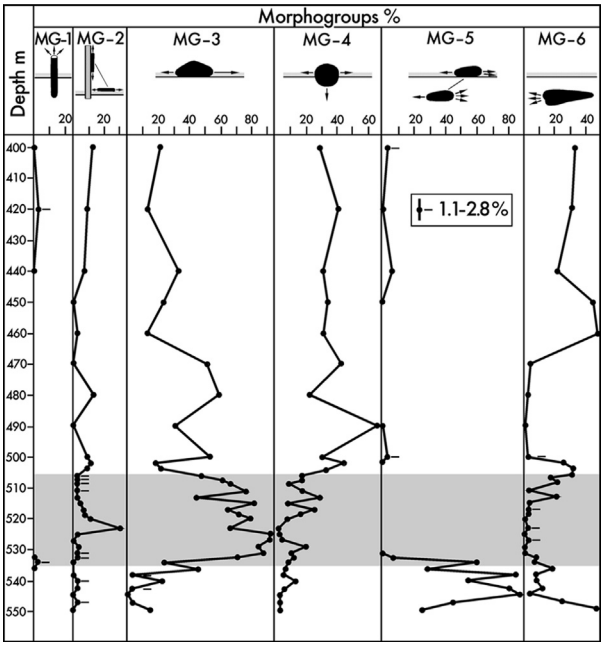

Fig. 8 Distribution of foraminiferal morphogroups (MGs) in the lower 150 m of core BH9/05. The Paleocene–Eocene Thermal Maximum (PETM) anomaly (shaded) is typified by high dominance of the surface-dwelling group MG-3.

in the lower part of the anomaly, but increases gradually in the upper part where it reaches 32%.

Through the post-anomaly interval, from 504 to 400 m, the most common MGs are the surficial MG-3 and the semi-immersed MG-4, ranging from 14 to 60% and from 23 to 69%, respectively. The infaunal MG-6 is also common, but shows a wide range of variation from 0 to 52%.

Biotic responses to PETM and adjacent events in Spitsbergen

The PETM in the Gilsonryggen prodelta facies

The Gilsonryggen Member of the Frysjaodden Formation, with the PETM close to its base, was deposited in a distal to proximal prodelta setting, in front of the prograding Battfjellet–Aspelintoppen delta system (Fig. 2). The foraminiferal diversities typifying the member are summarized by an alpha versus H(S) diagram (Fig. 9), the base graph of which principally accords with modern environments (Murray 2006; Nagy et al. 2011). The low diversity and almost entirely agglutinated nature of the assemblages indicate restricted environmental conditions throughout the whole member, but the most severe impact is seen within the PETM. Background data from the Paleogene Arctic Ocean also suggest that low salinity and reduced access to oxygen were most likely the main restricting factors.

The pre-PETM transgression

The deposition of the Gilsonryggen Member was initiated by a regional transgression. In the Nordenskiøldfjellet and Liljevalchfjellet sections, the sea encroached upon delta plain sandstones (with rootlet horizons), and in core BH9/05 it eroded in shoreface sandstones of the underlying Grumantbyen Formation. The sea-level rise culminated with maximum flooding, which deposited a distal prodelta shale package containing the PETM anomaly. The vertical distance between the transgressive surface and the PETM acme is 4.8 m on Nordenskiøldfjellet (Harding et al. 2011) and 19.8 m in core BH9/05. The sediments of this interval reveal an upwards-fining development as shown by the lithological log of core BH9/05 and decreasing quartz content in the Nordenskiøldfjellet section (Harding et al. 2011).

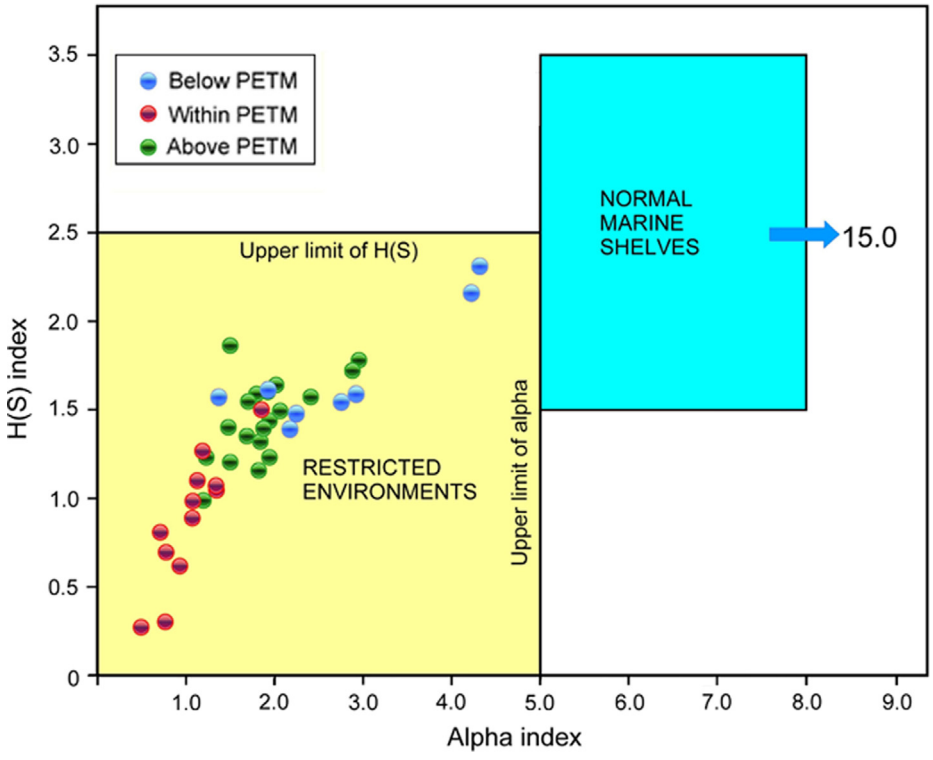

Fig. 9 Samples analysed from core BH9/05 plotted in an alpha versus H(S) diversity graph. All samples plot in the field of restricted environments. Samples from the Paleocene–Eocene Thermal Maximum (PETM) anomaly plot closest to the lower left corner suggesting highest restriction degree within the section.

Citation: *Polar Research* 2013, *32*, 19737, http://dx.doi.org/10.3402/polar.v32i0.19737

The PETM was associated with a eustatic sea-level rise of ca. 30 m (Sluijs et al. 2008), of which 3–5 m is regarded as steric rise, with the remainder ascribed to melting of alpine ice sheets in Antarctica (DeConto et al. 2012). In the Central Basin, this elevation is insufficient to explain the depth increase from subaerial exposure to maximum flooding that created offshore prodelta shelf conditions far below wave base. Moreover, the transgression started before the faunal turnover marking the onset of the PETM. Consequently, local tectonics has contributed significantly to the sea-level rise that culminated during the PETM.

The foraminiferal succession of the pre-PETM transgressive phase is composed of the FA 1 assemblage characterized by *R. arcticum* and consists of agglutinated taxa with very few calcareous forms (Fig. 5). The diversity is moderate with an average H(S) of 1.7. This, together with rare bioturbation (Fig. 3) of small-diameter traces, suggests a moderate hypoxia superimposed on a background of overall brackish conditions.

During the transgression, upwards-decreasing diversity suggests a gradual reduction in oxygenation with increasing water depth (Figs. 4, 6, 11). In accordance with this trend, the infaunal morphogroup MG-6 starts with a maximum in the lowermost part of the transgressive interval, which is followed by dominance of the semi-infaunal MG-5 showing peak values and then a strong upwards-reduction (Fig. 8). The overall hypoxia during the pre-PETM transgression was, however, too weak to give a significant size reduction, as shown by the high dominance of SAG-2 and -3, and presence of SAG-4 (Fig. 7).

The PETM anomaly

In core BH9/05, the onset of the PETM is well-marked by the sudden faunal turnover and associated diversity drop at 534.4 m (Figs. 5, 6). The diversity decreases further to the hyperthermal acme at 530.3 m, having a minimum H(S) value of 0.26. This is followed by an oscillating increase in diversity at least up to approximately 508.3 m, due to gradual immigration of new taxa. In this section too, the hyperthermal anomaly corresponds to a negative $\delta^{13}C$ excursion documented by Charles et al. (2011) and Cui et al. (2011). The FA 2 occupying the anomaly interval shows extremely low diversities with an average H(S) of 0.9 and strong dominance of the small-sized *Trochammina* aff. *inornata* (average 70%), suggesting severely reduced benthic oxygenation.

The faunal turnover at the base of the PETM is marked by the last occurrence of the dominant species of FA 1, *R. arcticum* and *L. turbida*, as well as other taxa including *R. borealis*, *Reticulophragmium* sp. 1, *Convallina* aff. *elongata*, *Verneuilinoides* sp.1 and *Verneuilinoides* aff. *durus* (Fig. 5). This fauna is replaced with high abundance of *Trochammina*, dominating assemblage FA 2. In the Beaufort–Mackenzie Basin, Arctic Canada, a similar turnover leads to replacement of *Reticulophragmium* assemblages with faunas heavily dominated by *Trochammina*. This turnover has been dated to the latest Paleocene (McNeil 1996, 1997), but faunal similarities to the Spitsbergen assemblages suggest a younger age, correlative with the onset of the PETM.

In core BH9/05, the PETM anomaly is occupied by the size group SAG-1, strongly dominated by very small foraminifera with an average of 79.2% (Fig. 7). This indicates that hypoxia was a significant restricting factor; a view supported by the observation that reduced foraminiferal test dimensions are typical of numerous modern hypoxic faunas (Bernhard & Sen Gupta 1999). It is a widely held opinion that this feature has a double function. Small size means an increase of the body surface area relative to volume, enhancing oxygen uptake. In addition, small size reflects a rapid reproduction rate, which is a feature of opportunistic taxa adapted to rapidly changing conditions where fast recolonization is an advantage.

Adaptation of small-sized *Trochammina* (similar to *T.* aff. *inornata* of the Spitsbergen PETM) to low oxygen conditions is exemplified by modern faunas of the Aso-Kai Lagoon (Japan), and Late Triassic to Early Jurassic delta-influenced assemblages of Spitsbergen (Nagy, Hess et al. 2010). Increased abundance of small-sized benthic foraminifera is reported from the PETM by Thomas (1998) and Galeotti et al. (2004).

MG analysis shows that the FA of the PETM interval (534.4–504.0 m) consists mainly of the surficial MG-3 averaging 80%, while the remainder is almost entirely made up of the epifaunal MG-2 and semi-immersed MG-4 (Fig. 8). The infaunal MG-6 is rare ($<3.4\%$) to absent. This combination suggests that the redox boundary was at the sediment–water interface, which allowed development of a large surficial component but severely restricted the infauna. Above 509 m, MG-4 and -6 increase in abundance, with a corresponding reduction of MG-3, suggesting a gradually enhancing oxygenation of the sea floor.

The laminated, non-bioturbated shales deposited during the PETM and the subsequent recovery period agree with this interpretation of severe near-bottom hypoxia (Figs. 3, 11). The fossil- and lithology-based evidence of hypoxia corresponds to the strongly reduced thorium/uranium ratio (Fig. 10) recognized across the PETM anomaly by Dypvik et al. (2011). It reflects the

higher potential of uranium (compared to thorium) to precipitate under oxygen-depleted conditions. Thus, faunal, lithological and geochemical proxies agree that peak hypoxia during the PETM of the palaeo-Arctic Ocean also extended to its marginal seas.

As previously described, low salinity was a general feature of the Paleocene–Eocene Arctic Ocean and particularly its marginal extensions such as the Central Basin. Superimposed on these background conditions, a further salinity reduction may have occurred during the PETM, as suggested by a strongly increased kaolinite content reported from Spitsbergen (Dypvik et al. 2011). This phenomenon (Fig. 10) is indicative of enhanced continental weathering under a warm and humid climate with an intensified hydrological cycle. In the marine realm, increased freshwater influx led to strengthened salinity stratification of the waters, amplifying the tendency to hypoxia.

In the southern Barents Sea, the PETM is marked by occurrence of *A. augustum*, which in the commercial well 7119/9-1 ranges from 1100 to 880 m (Nagy et al. 1997). This range coincides with a wide acme of deep-water agglutinated foraminifera, belonging mainly to the genus *Rhizammina*, suggesting a middle bathyal water depth. The acme corresponds to the middle part of a deep-water faunal succession revealing a transgressive–regressive development from 1300 to 720 m. No faunal turnover or diversity change is observed within the acme, which suggests that strongly increased water depth during the transgression has faded out the effects of the PETM in these basinal environments.

The post-anomaly regression with facies trend change

Above the PETM, from 504 to 360 m, the foraminiferal diversity further increases (Figs. 4, 6, 11), and the assemblages develop similar abundance of the epifaunal MG-3, semi-immersed MG-4 and later the infaunal MG-6 (Fig. 8). This suggests enhanced oxygenation of the water column, although bottom-water hypoxia remains a dominant restricting factor as indicated by continuing absence of bioturbation. Several new foraminiferal taxa appear through this interval, where the dominant species is *Reophax* aff. *metensis*, followed in abundance by *Trochammina* aff. *inornata* and *Thurammina* aff. *papillata* (Fig. 5). This interval apparently represents the recovery period after the hyperthermal event, superimposed on a gradual shallowing of the basin.

In the middle of the Gilsonryggen Member, diversity maxima appear at 340 and 280 m, with alpha values of 2.9 and 2.8, respectively (Figs. 4, 6). In addition, this interval contains dense bioturbation by small-sized (2 mm diameter) traces of *Chondrites*-type, confined to numerous thin beds (1–3 cm). The combination of these features reflects a facies trend change (Figs. 3, 11), where hypoxia is replaced by low salinity as the most significant restricting factor.

Delta progradation effects. The upper part of the Gilsonryggen Member shows an upwards-coarsening lithology leading to trough cross-bedded sandstones in the topmost part. This influx of coarse-grained material reflects the progradation of the Battfjellet–Aspelintoppen

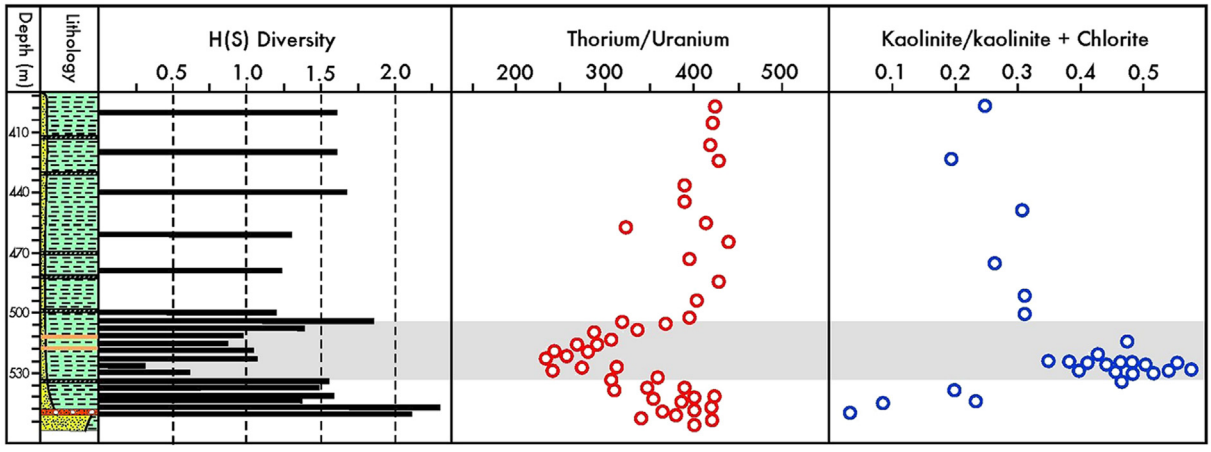

Fig. 10 Distribution of environmental proxies in core BH9/05 including H(S) diversity index, thorium/uranium ratio and kaolinite content. The Paleocene–Eocene Thermal Maximum (PETM) anomaly is shaded. (The plots of the latter two proxies are based on data from Dypvik et al. 2011.)

Citation: *Polar Research* 2013, *32*, 19737, http://dx.doi.org/10.3402/polar.v32i0.19737

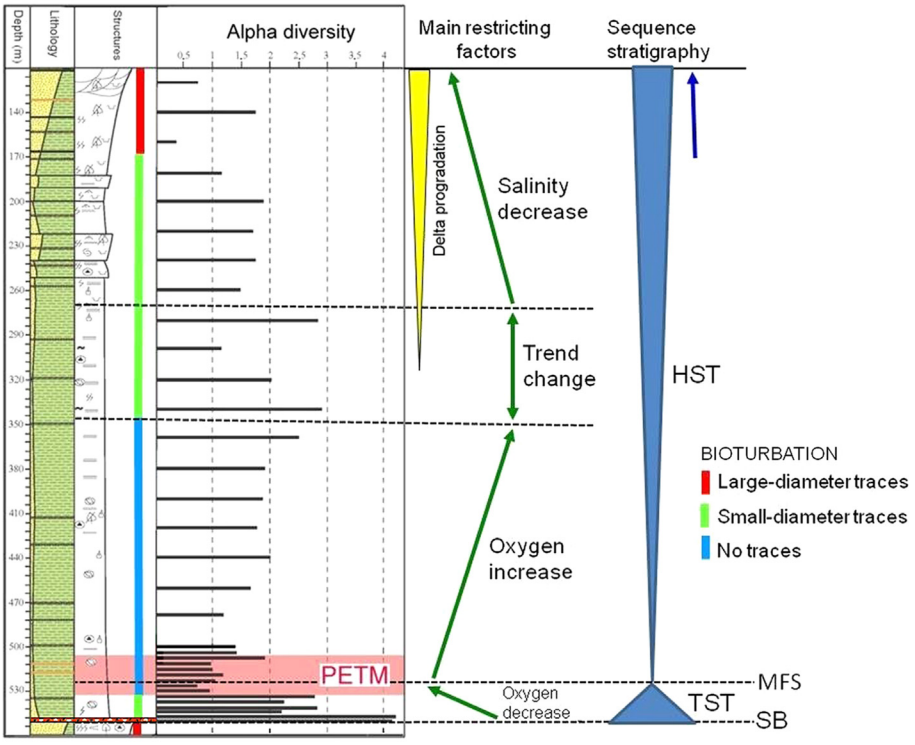

Fig. 11 Outline of biofacies trends combined with sequence stratigraphy of core BH9/05. The following terms are abbreviated: sequence boundary (SB), transgressive systems tract (TST), maximum flooding surface (MFS) and highstand systems tract (HST).

delta system (Fig. 11). Upwards-improving oxygenation is indicated by enhanced bioturbation with expanding diameter of the mostly horizontal traces (Fig. 3). These features are accompanied by an upwards-decrease in foraminiferal diversity, probably due to the increasing effects of deltaic discharge that culminated in the delta front to coastal facies of the overlying Battfjellet to Aspelintoppen formations (Fig. 2).

The Spitsbergen PETM in a sequence stratigraphic framework

Transgressive systems tract

The studied interval of core BH9/05 represents the most marine lower part of the Gilsonryggen sequence (Fig. 2). The conglomerate at the base of the Gilsonryggen Member depicts the transgressive surface and sequence boundary (SB) (Fig. 11). The succeeding thin transgressive systems tract (TST) reveals a weak fining-upwards lithology, accompanied by decreasing foraminiferal diversity as well as diminishing abundance of infaunal and semi-infaunal MGs, in accordance with increasing water depth coupled with decreasing oxygenation. In the Nordenskiøldfjellet section, a similar fining-upwards is evident in the basal Gilsonryggen shales, which rest on delta plain sandstones with rootlets forming the top of the Hollendardalen Member (Rüther 2007).

Maximum flooding

Both in core BH9/05 (Nagy, Dypvik et al. 2010) and in the Nordenskiøldfjellet section (Harding et al. 2011), the MFS of the Gilsonryggen sequence coincides within the PETM acme. At these sites, the transgression started before the onset of the PETM, and there is a large depth difference between the transgressive surface and the maximum flooding event (representing subaerial exposure and offshore shelf, respectively). These observations suggest that in Spitsbergen the PETM-induced eustatic sea-level rise was superimposed on a significant basin subsidence. The combined effect of these two bathymetric factors significantly increased the water depth, which led to increasing intensity of hypoxia, particularly in the near-bottom waters. The hypoxia was amplified by the thermohaline stratification of the water column due mainly to the warm and humid climate.

Highstand systems tract

The main body of the Gilsonryggen Member above the MFS belongs to the highstand systems tract (HST) (Fig. 11), which extends upwards through the coarsening-upwards transitional prodelta beds, continuing in the overlying delta front sandstones of the Battfjellet Formation and terminating in the delta plain mudstones and sandstones of the Aspelintoppen Formation.

The HST within the Gilsonryggen Member comprises three segments as defined mainly by biofacies developments (Fig. 11). In the lower segment, extending upwards from the maximum flooding, upwards-increasing oxygenation appears to have been the main restricting factor. The middle segment represents a biofacies trend change zone, where the restricting effect of low oxygen is replaced by low salinity as the dominant factor. In the upper segment, decreasing salinity prevails as the main restricting factor, coupled with delta progradation.

Conclusions

This study applies benthic foraminiferal proxies to display palaeoenvironmental changes and stratigraphic developments across the PETM and adjacent strata in the Palaeogene Central Basin of Spitsbergen. The impact of this transient period of intensive global warming here is recognized in prodelta shelf mudstones comprising the lower part of the Gilsonryggen Member (of the Frysjaodden Formation). The faunal analyses are based on SNSG core BH9/05, which contains benthic FA in a continuous succession composed (almost exclusively) of agglutinated taxa.

The deltaic marine Central Basin succession was deposited in a potentially brackish environment with a tendency to hypoxia. The effects of the PETM were superimposed on and amplified these tendencies, leading to significant biotic changes in the benthic realm.

In core BH9/05, the climatic perturbation started with a faunal turnover marked by the disappearance of the relatively high-diversity *Reticulophragmium* assemblage, and its abrupt replacement by an extremely low-diversity *Trochammina* fauna that typifies the PETM and the subsequent recovery period. The turnover was also recognized in other marginal basins of the palaeo-Arctic Ocean and appears to have a circumpolar extent.

Extremely low species diversities across the PETM anomaly are explained by the increased effects of low salinity and bottom-water oxygen depletion in a thermohaline-stratified water column. Additional proxies for oxygenation based on benthic foraminifera are changes in test surface area and MG distribution pattern. During the PETM, distinctly increased bottom-water hypoxia is indicated by a high dominance of species with a small surface area, living epifaunally as the sediment pore water became too anoxic to harbour foraminifera.

Geochemical data from core BH9/05 published by Dypvik et al. (2011) agrees with the assessment of reduced salinity and oxygenation based on foraminifera. At the PETM anomaly, increased kaolinite content suggests increased fluvial discharge to the Central Basin, due to intensification of the hydrological cycle during global warming. Strongly reduced thorium/uranium ratios at the anomaly signal decreased oxygenation.

In a sequence stratigraphic framework, the lowermost part of the Gilsonryggen Member represents the TST extending from the transgressive surface (SB) and culminating with maximum flooding, which coincides with the PETM acme. Increasing water depth during the transgression is evidenced by fining-upwards lithology coeval with decreasing oxygenation. The transgression appears to be the combined effect of local tectonic subsidence and a superimposed eustatic sea-level rise driven by the PETM oceanic warming and potentially melting glaciers on Antarctica.

The HST comprises the main body of the Gilsonryggen Member and continues further upwards. The recovery phase following the PETM is developed in the lowermost part of this systems tract, reflecting upwards enhancing oxygenation. After a biofacies trend change, upwards decrease in salinity becomes the main restricting factor, accompanying the progradation of the Battfjellet–Aspelintoppen delta system.

Acknowledgements

The authors thank Store Norske Spitsbergen Grubekompani for providing samples from drill core BH9/05 and for giving us access to logging facilities in their core store. Jonna Poikolainen is thanked for important assistance during the core logging and Adam Charles for useful discussions. Appreciation is extended to members of the pACE group and, particularly, its co-ordinator Tim White, for an inspiring field trip and meetings. We acknowledge numerous corrections and suggestions from Ellen Thomas, which significantly improved this article. Valuable comments were also provided by Jaroslaw Tyszka and the referees Laia Alegret and Michael Kaminski.

References

Alegret L., Ortiz S., Arenillas I. & Molin E. 2010. What happens when the ocean is overheated? The foraminiferal response across the Paleocene–Eocene Thermal Maximum

Citation: *Polar Research* 2013, *32*, 19737, http://dx.doi.org/10.3402/polar.v32i0.19737

at the Alamedilla section (Spain). *Geological Society of America Bulletin 122*, 1616–1624.

Aziz H.A., Hilgen F.J., Van Luijk G.M., Sluijs A., Kraus M.J., Pares J.M. & Gingerich P.D. 2008. Astronomical climate control on paleosol stacking patterns in the upper Paleocene–lower Eocene Willwood Formation, Bighorn Basin, Wyoming. *Geology 36*, 531–534.

Bernhard J.M. & Sen Gupta B.K. 1999. Foraminifera in oxygen-depleted environments. In B.K. Sen Gupta (ed.): *Modern foraminifera*. Pp. 201–216. Dordrecht: Kluwer.

Bowen G.J., Beerling D.J., Koch P.L., Zachos J.C. & Quattlebaum T. 2004. A humid climate state during the Palaeocene/Eocene Thermal Maximum. *Nature 432*, 495–499.

Briggs J.C. 1987. *Biogeography and plate tectonics. Developments in palaeontology and stratigraphy 10*. Amsterdam: Elsevier Scientific Publishers.

Brinkhuis H., Schouten S., Collinson M.E., Sluijs A., Sinninghe Damste J.S., Dickens G.R., Humber M., Cronin T.M., Onodera J., Takahashi K., Bujak J.P., Stein R., Van der Burgh J., Eldrett J.S., Harding I.C., Lotter A.F., Sangiorgi F., Van Konijnenburg-Van Cittert H., De Leeuw J.W., Matthiessen J., Beckman J., Moran K. & The Expedition 302 Scientists. 2006. Episodic fresh surface water in the Eocene Arctic Ocean. *Nature 441*, 606–609.

Buzas M.A. & Gibson T.G. 1969. Species diversity: benthic foraminifera in western North Atlantic. *Science 163*, 72–75.

Charles A.J., Condon D.J., Harding I.C., Pälike H., Marshall J.E.A., Cui Y., Kump L. & Croudance I.W. 2011. Constraints on the numerical age of the Paleocene–Eocene boundary. *Geochemistry, Geophysics, Geosystems 12*, Q0AA17, doi: 10.1029/2010GC003426.

Crouch E.M., Heilman-Clausen C., Brinkhuis H., Morgans H.E.G., Rogers K.M., Egger H. & Schmitz B. 2001. Global dinoflagellate event associated with the Paleocene Thermal Maximum. *Geology 29*, 315–318.

Cui Y., Kump L.R., Ridgwell A.J., Charles A.J., Junium C.K., Diefendorf A.F., Freeman K.H., Urban N.M. & Harding I.C. 2011. Slow release of fossil carbon during the Paleocene–Eocene Thermal Maximum. *Nature Geoscience 4*, 481–485.

Dallmann W.K., Midbø P.S., Nøttvedt A. & Steel R.J. 1999. Tertiary lithostratigraphy. In W.K. Dallmann (ed.): *Lithostratigraphic lexicon of Svalbard*. Pp. 215–263. Tromsø: Norwegian Polar Institute.

DeConto R.M., Galleotti S., Pagani M., Tracy D., Schafer K., Zhang T., Pollard D. & Beerling D.J. 2012. Past extreme warming events linked to massive carbon release from the warming permafrost. *Nature 484*, 87–91.

Dickens G.R., O'Neil J.R., Rea D.K. & Owen R.M. 1995. Dissociation of oceanic methane as a cause of carbon isotope excursion at the end of the Paleocene Thermal Maximum. *Paleoceanography 10*, 965–971.

Dypvik H., Riber L., Burca F., Rüther C.D., Jargvoll D. & Nagy J. 2010. Mineralogical shifts at the Paleocene–Eocene Thermal Maximum (PETM) event, Svalbard. In H.A. Nakrem et al. (eds.): *Abstracts and proceedings, 29th Nordic Geological Winter Meeting*. P. 42. Trondheim: Geological Society of Norway.

Dypvik H., Riber L., Burca F., Rüther D., Jargvoll D., Nagy J. & Jochmann M. 2011. The Paleocene–Eocene Thermal Maximum in Svalbard—clay mineral and geochemical signals. *Palaeogeography, Palaeoclimatology, Palaeoecology 303(3–4)*, 156–169.

Galeotti S., Kaminski M.A., Coccioni R. & Speier R. 2004. High resolution deep water agglutinated and calcareous hyaline foraminiferal record across the Paleocene/Eocene transition in the Contessa Road section (central Italy). In M. Bubik & M.A. Kaminski (eds.): *Proceedings of the Sixth International Workshop on Agglutinated Foraminifera. Grzubowski Foundation Special Publication 8*. Pp. 83–103. Krakow: Grzybowski Foundation.

Harding I.C., Charles A.J., Marshall J.E.A., Pälike H., Roberts P.A., Wilson P.A., Jarvis E., Thorne R., Morris E., Moremon R., Pearce R.B. & Akbari S. 2011. Sea level and salinity fluctuations during the Paleocene–Eocene Thermal Maximum in Arctic Spitsbergen. *Earth and Planetary Science Letters 303*, 97–107.

Harland W.B. 1997. *The geology of Svalbard. Memoir 17*. London: Geological Society.

Jakobsson M., Backman J., Rudels B., Nycander J., Frank M., Mayer L., Jokat W., Sangiorgi F., O'Regan M., Brinkhuis H. & Moran K. 2007. The Early Miocene onset of a ventilated circulation regime in the Arctic Ocean. *Nature 447*, 986–990.

Jones R.W. & Charnock M.A. 1985. Morphogroups of agglutinating foraminifera. Their life position, feeding habits and potential applicability in (paleo)ecological studies. *Revue de Paleobiologie 4*, 311–320.

Jorissen F.J., De Stigter H.C. & Widmark J.G.V. 1995. A conceptual model explaining benthic foraminiferal microhabitats. *Marine Micropaleontology 26*, 3–15.

Kaminski M.A. & Gradstein F.M. 2005. *Atlas of Paleogene cosmopolitan deep-water agglutinated foraminifera. Grzubowski foundation special publication 10*. Krakow: Grzubowski Foundation.

Kaminski M.A., Silye L. & Kender S. 2009. Miocene deep-water agglutinated foraminifera from the Lomonosov Ridge and opening of the Fram Strait. *Micropaleontology 55*, 117–135.

Kelly D.C., Bralower T.J., Zachos J.C., Premoli-Silva I. & Thomas E. 1996. Rapid diversification of planktonic foraminifera in the tropical Pacific (ODP site 865) during the late Paleocene Thermal Maximum. *Geology 24*, 423–426.

Kennett J.P. & Scott L. 1991. Abrupt deep-sea warming, palaeoceanographic changes and benthic extinctions at the end of the Palaeocene. *Nature 353*, 225–229.

Magioncalad R., Dupuis C., Smith T., Steuerbaut E. & Gingerish P.D. 2004. Paleocene–Eocene carbon isotope excursion in organic carbon and pedogenic carbonate: direct comparison in a continental stratigraphic section. *Geology 32*, 553–556.

Manum S.B. & Throndsen T. 1986. Age of Tertiary formations on Spitsbergen. *Polar Research 4*, 103–131.

McNeil D.H. 1990. Tertiary marine events of the Beaufort–Mackenzie Basin and correlation of Oligocene to Pliocene marine outcrops in Arctic North America. *Arctic 43*, 301–313.

McNeil D.H. 1996. Distribution of Cenozoic agglutinated benthic foraminifera in the Beaufort–Mackenzie Basin. In J. Dixon (ed.): *Geological atlas of the Beaufort–Mackenzie area. Geological Survey of Canada, Miscellaneous Report 59*. Fig. 70. Calgary: Geological Survey of Canada.

McNeil D.H. 1997. *New foraminifera from the Upper Cretaceous and Cenozoic of the Beaufort–Mackenzie Basin of Arctic Canada. Cushman Foundation of Foraminiferal Research, special publication 35*. Cambridge, MA: Cushman Foundation of Foraminiferal Research.

Moran K., Backman J., Brinkhuis H., Clemens S., Cronin T., Dickens G., Eynaud F., Gattacceca J., Jakobsson M., Jordan R., Kaminski M., King J., Koc N., Krylov A., Martinez N., Matthiessen J., McInroy D., Moore T., Onodera J., O'Regan M., Pälike H., Rea B., Rio D., Sakamoto T., Smith D., Stein R., St John C., Suto I., Suzuki N., Takahashi K., Watanabe M., Yamamoto M., Farrell J., Frank M., Kubik P., Jokat W. & Kristoffersen Y. 2006. The Cenozoic palaeoenvironment of the Arctic Ocean. *Nature 441*, 601–605.

Murray J.W. 1973. *Distribution and ecology of living benthic foraminiferids*. London: Heinemann Educational Books.

Murray J.W. 2006. *Ecology and applications of benthic foraminifera*. New York: Cambridge University Press.

Nagy J. 1992. Environmental significance of foraminiferal morphogroups in Jurassic North Sea deltas. *Palaeogeography, Palaeoclimatology, Palaeoecology 95*, 111–134.

Nagy J. 2005. Delta-influenced foraminiferal facies and sequence stratigraphy of Paleocene deposits in Spitsbergen. *Palaeogeography, Palaeoclimatology, Palaeoecology 222*, 161–179.

Nagy J., Dypvik H., Jargvoll D. & Riber L. 2010. Features of a semi-isolated Arctic Ocean and the Paleocene–Eocene Thermal Maximum (PETM) reflected in the Paleogene foraminiferal facies of Spitsbergen. In H.A. Nakrem et al. (eds.): *Abstracts and proceedings, 29th Nordic Geological Winter Meeting*. P. 131. Trondheim: Geological Society of Norway.

Nagy J., Gradstein F.M., Kaminski M.A. & Holbourn A.E. 1995. Foraminiferal morphogroups, paleoenvironments and new taxa from Jurassic and Cretaceous strata of Thakola, Nepal. In M.A. Kaminski et al. (eds.): *Proceedings of the Fourth International Workshop on Agglutinated Foraminifera. Grzybowski Foundation Special Publication 3*. Pp. 181–209. Krakow: Grzybowski Foundation.

Nagy J., Hess S. & Alve E. 2010. Environmental significance of foraminiferal assemblages dominated by small-sized Ammodiscus and Trochammina in Triassic and Jurassic delta-influenced deposits. *Earth-Science Reviews 99*, 31–49.

Nagy J., Hess S., Dypvik H. & Bjærke T. 2011. Marine shelf to paralic biofacies of Upper Triassic to Lower Jurassic deposits in Spitsbergen. *Palaeogeography, Palaeoclimatology, Palaeoecology 300*, 138–151.

Nagy J., Kaminski M.A., Johnsen K. & Mitlehner A.G. 1997. Foraminiferal, palynomorph, and diatom biostratigraphy and paleoenvironments of the Torsk Formation: a reference section for the Paleocene–Eocene transition in the western Barents Sea. In H.C. Hass & M.A. Kaminski (eds.): *Contributions to the micropaleontology and paleoceanography of the northern North Atlantic. Grzybowski Foundation Special Publication 5*. Pp. 15–38. Krakow: Grzybowski Foundation.

Nagy J., Kaminski M.A., Kuhnt W. & Bremer M. 2000. Agglutinated foraminifera from neritic to bathyal facies in the Paleogene of Spitsbergen and the Barents Sea. In M.B. Hart et al. (eds.): *Proceedings of the Fifth International Workshop on Agglutinated Foraminifera, Grzybowski Foundation Special Publication 7*. Pp. 333–361. Krakow: Grzybowski Foundation.

Ogawa Y., Takahashi K., Yamanaka T. & Onodera J. 2009. Significance of euxinic conditions in the middle Eocene paleo-Arctic basin: a geochemical study of the IO Arctic Coring Expedition 302 sediments. *Earth and Planetary Science Letters 285*, 190–197.

Pagani M., Pedentchouk N., Huber M., Sluijs A., Brinkhuis H., Sinninghe Damsté J.S., Dickens G.R. & Expedition 302 scientists. 2006. Arctic hydrology during global warming at the Paleocene/Eocene Thermal Maximum. *Nature 422*, 671–675.

Podobina V.M. 2000. Paleogene agglutinated foraminifera of the western Siberian biogeographical province. In M.B. Hart et al. (eds.): *Proceedings of the Fifth International Workshop on Agglutinate Foraminifera, Grzyb Foundation Special Publication 7*. Pp. 387–396. Krakow: Grzybowski Foundation.

Reolid M., Rodriguez-Tovar F.J., Nagy J. & Oloriz F. 2008. Benthic foraminiferal morphogroups of mid to outer shelf environments of the Late Jurassic (Prebethic Zone, southern Spain): characterization of biofacies and environmental significance. *Palaeogeography, Palaeoclimatology, Palaeoecology 261*, 280–299.

Röhl U., Westerhold T., Barlower T.J. & Zachos J.C. 2007. On the duration of the Paleocene–Eocene Thermal Maximum (PETM). *Geochemistry, Geophysics, Geosystems 8*, Q12002, doi: 10.1029/2007GC001784.

Rüther C.D. 2007. *Delta-influenced Paleogene depositional environments of the Frysjaodden and Hollendardalen formations*. Master thesis, University of Oslo.

Setoyama E., Kaminski M.A. & Tyszka J. 2011. The Late Cretaceous–Early Paleocene palaeobathymetric trends in the southwestern Barents Sea—palaeoenvironmental implications of benthic foraminiferal assemblage analysis. *Palaeogeography, Palaeoclimatology, Palaeoecology 307*, 44–58.

Sluijs A., Schouten S., Pagani M., Woltering M., Brinkhuis H., Sinninghe Damsté J.S., Dickens G.R., Huber M., Reichart G.J., Stein R., Matthiessen J., Lourens L.J., Pedentchouk N., Backman J., Moren, K. & Expedition 302 scientists. 2006. Subtropical Arctic ocean temperatures during the Palaeocene/Eocene Thermal Maximum. *Nature 441*, 610–613.

Sluijs A., Brinkhuis H., Crouch E.M., John C.M., Handley L., Munsterman D., Bohaty S.M., Zachos J.C., Reichart G., Schouten S., Pancost R.D., Sinninghe Damsté J., Welters N.L.D., Lotter A.F. & Dickens G.R. 2008. Eustatic variations

Citation: *Polar Research* 2013, *32*, 19737, http://dx.doi.org/10.3402/polar.v32i0.19737

during the Palaeocene–Eocene greenhouse world. *Paleoceanography 23*, PA4216, doi: 10.1029/2008PA001615.

Smith T., Rose K.D. & Gingerich P.D. 2006. Rapid Asia–Europe–North America geographic dispersal of earliest Eocene primate Teilhardina during the Paleocene–Eocene Thermal Maximum. *Proceedings of the National Academy of Sciences of the United States of America 103*, 11223–11227.

Steel R.J., Gjelberg J., Helland-Hansen W., Kleinsphen K., Noettvedt A. & Rye Larsen M. 1985. The Tertiary strike–slip basins and orogenic belt of Spitsbergen. In K.T. Biddle & N. Christie-Blick (eds.): *Strike–slip deformation, basin formation and sedimentation. Special publication 37.* Pp. 339–359. Tulsa: Society of Economic Paleontologists and Mineralogists.

Svensen H., Planke S., Malthe-Sørenssen A., Jamtveit B., Myklebust R., Eidem T.R. & Rey S.S. 2004. Release of methane from a volcanic basin as a mechanism for initial Eocene global warming. *Nature 429*, 542–545.

Thomas D.J., Bralower T.J. & Zachos T.J. 1999. New evidence for subtropical warming during the late Paleocene Thermal Maximum: stable isotopes from Deep Sea Drilling Project Site 527, Walvis Ridge. *Paleoceanography 14*, 561–570.

Thomas E. 1998. Biogeography of the late Paleocene benthic foraminiferal extinction. In M.P. Aubry et al. (eds.): *Late Paleocene–early Eocene biotic and climatic events in the marine and terrestrial records*. Pp. 214–243. New York: Columbia University Press.

Thomas E. & Shackelton N.J. 1996. The Paleocene-Eocene benthic foraminiferal extinction and stable isotope anomalies. In R.W. Knox et al. (eds.): *Correlation of the early Paleogene in Northwest Europe. Special publication 101*. Pp. 401–441. London: Geological Society.

Westerhold T., Röhl U., McKarren H.K. & Zachos J.C. 2009. Latest on the absolute age of the Paleocene–Eocene Thermal Maximum (PETM): new insight from exact stratigraphic position of key ash layers + 19 and −17. *Earth and Planetary Science Letters 287*, 412–419.

Wing S.L., Harrington G.J., Smith F.A., Bloch J.I., Boyer D.M. & Freeman K.H. 2005. Transient floral change and rapid global warming at the Paleocene–Eocene boundary. *Science 310*, 993–996.

Zachos J.C., Pagani M., Sloan L., Thomas E. & Billups K. 2001. Trends, rhythms and aberrations in global climate 65 Ma to present. *Science 292*, 686–693.